



**HAL**  
open science

## Experimental study of the autoxidation of n-dodecane and 1,2,4-trimethylbenzene

Soraya Aminane, Mickaël Sicard, Frédéric Ser, Lorette Sicard

► **To cite this version:**

Soraya Aminane, Mickaël Sicard, Frédéric Ser, Lorette Sicard. Experimental study of the autoxidation of n-dodecane and 1,2,4-trimethylbenzene. IASH 2019, Sep 2019, LONG BEACH, United States. hal-02507862

**HAL Id: hal-02507862**

**<https://hal.science/hal-02507862v1>**

Submitted on 13 Mar 2020

**HAL** is a multi-disciplinary open access archive for the deposit and dissemination of scientific research documents, whether they are published or not. The documents may come from teaching and research institutions in France or abroad, or from public or private research centers.

L'archive ouverte pluridisciplinaire **HAL**, est destinée au dépôt et à la diffusion de documents scientifiques de niveau recherche, publiés ou non, émanant des établissements d'enseignement et de recherche français ou étrangers, des laboratoires publics ou privés.

***IASH 2019, the 16<sup>TH</sup> INTERNATIONAL CONFERENCE ON  
STABILITY, HANDLING AND USE OF LIQUID FUELS  
Long Beach, California USA  
8-12 September 2019***

**EXPERIMENTAL STUDY OF THE AUTOXIDATION OF  
n-DODECANE AND 1,2,4-TRIMETHYLBENZENE**

Soraya Aminane<sup>1</sup>, Mickaël Sicard<sup>1</sup>, Frédéric Ser<sup>1</sup>, Lorette Sicard<sup>2</sup>

<sup>1</sup> DMPE, ONERA Université Paris Saclay, Palaiseau, F-91123, France,  
[soraya.aminane@onera.fr](mailto:soraya.aminane@onera.fr)

<sup>2</sup> Laboratoire ITODYS, 15 Rue Jean Antoine de Baïf, 75013 Paris, France

During its course in the fuel system, the fuel is subjected to thermal stress, leading to the formation of solid deposits in the fuel system and injectors, and thus causing clogging phenomena and a malfunction of these devices.

The notion of thermal stability, which in some cases is illustrated by the formation of solid deposits in jet fuel, is related to the chemical composition and the presence of oxygen naturally dissolved in fuel. However, the understanding of oxidative fuel degradation is based on little known autoxidation mechanisms.

Experimentally, the investigation of the oxidation sensitivity of jet fuel is carried out using the PetroOXY device, thanks to model molecules of linear alkane and monoaromatic type, *n*-dodecane (*n*-C<sub>12</sub>) and 1,2,4-Trimethylbenzene (1,2,4-TMB), respectively. First, the model molecules are studied pure in order to highlight their behavior under thermo-oxidative stresses. Secondly, these molecules were mixed in proportion 80 % *n*-dodecane /20 % 1,2,4-TMB, in order to model a fuel surrogate.

Beyond a color change (colorless to yellow), the results revealed that the induction period is significantly lower for the pure molecules whereas for the mixture, the induction time is doubled. Moreover, the appearance of a gel, probably a precursor of solid deposits is observed, showing clearly the interactions between the molecules.

The mechanisms involved during this process were determined using several analytical characterization techniques (GC, GC/MS) allowing us to identify the products of oxidation formed but also the quantification of them using chemical techniques (Peroxide Value, Total Acid Number, water content).

**KEYWORDS:** Hydrocarbons, thermo-oxidative mechanisms, RSSOT

## INTRODUCTION

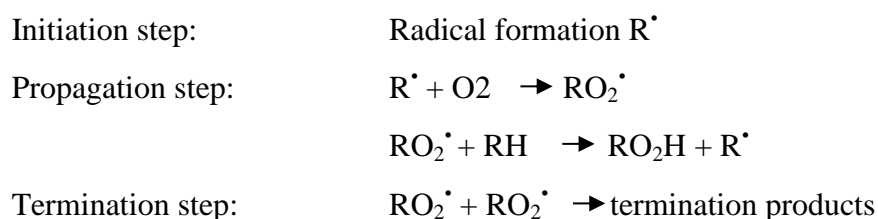
Jet fuel, although used primarily to give energy to the aircraft engine, can also serve as a coolant. As a result, it can reach temperatures above 200 °C. This thermal stress leads to the degradation of the fuel, producing in some case the formation of deposits in fuel systems and injectors. The formation of such deposits results in a loss of thermal transfer efficiency and can lead to malfunction of the injectors, whose mission is to reduce NO<sub>x</sub> and CO<sub>2</sub> emissions. This implies regular cleanings and would thus be at the origin of immobilization of commercial aircrafts. The thermal stability of jet fuel is thus the linked to economic and environmental criteria. Thermal stability refers to the tendency of a fuel to degrade and form deposits according to the temperature range to which it is subjected.<sup>1, 2</sup> Thus, under the effect of temperature, this term includes two phenomena: autoxidation and thermal cracking.

Autoxidation occurs at moderate temperatures between 140 and 250 ° C, and results from the complex interaction between dissolved oxygen and hydrocarbon molecules. Indeed, when the fuel is in contact with the air, the oxygen present in the atmosphere dissolves naturally in the fuel and reacts to form free radicals, which initiate and propagate autoxidation reactions.<sup>3-8</sup>

Thus, the formation of solid deposits in fuels results initially from autoxidation reactions, which act as radical precursors and in a second phase reactions of thermal decomposition of fuels.<sup>9</sup> In our study, we focus exclusively on autoxidation reactions.

## BACKGROUND

It is generally accepted that the autoxidation process proceeds through a radical-type mechanism involving dissolved oxygen. Zabarnick (1993)<sup>10</sup> proposed a mechanism to describe the oxidation of fuels which was inspired by the oxidation mechanism at low-temperature. Heneghan (1994)<sup>11</sup> then proposed that the autoxidation mechanism can be detailed as follows:



where RH is a hydrocarbon representing an aliphatic chain of alkane type, R<sup>•</sup> is the hydrocarbon alkyl radical, RO<sub>2</sub><sup>•</sup> is the peroxide radical, RO<sub>2</sub>H is a hydroperoxide.

A pseudo-detailed mechanism, given in *Figure 1*, was recently reported by Kuprowicz *and al.*<sup>12</sup> and West 13.

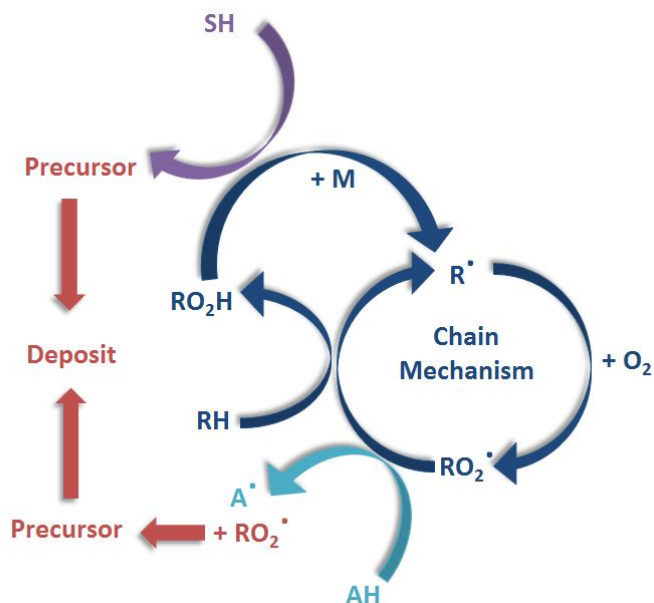


Figure 1 - Pseudo-detailed mechanism of fuel autoxidation

In this cyclic mechanism, a first initiation reaction consists in the hydrogen atom abstraction from a carbon atom to form an alkyl radical  $R^\bullet$ . The alkyl radical reacts rapidly with dissolved diatomic oxygen, to very quickly form an alkyl peroxide radical  $RO_2^\bullet$ . The latter is not as reactive as the carbon free radical, but is sufficiently reactive to remove another hydrogen from a carbon to form a hydroperoxide  $RO_2H$  and regenerate another alkyl radical  $R^\bullet$ , thus propagating the cycle of the chain. The new carbon free radical formed can then again react with the oxygen to continue the propagation cycle. This chain reaction ends when two free radicals react with each other, this constitutes the termination step. Antioxidants (AH) and SH reactive sulfur species can also interfere in the process.<sup>8, 14</sup>

Various studies have highlighted the oxidation products resulting from autoxidation reactions of alkanes.<sup>2, 15, 16, 17-20, 21, 22-30</sup>

Indeed, the hydroperoxides, the primary oxidation products, degrade to form secondary oxidation products, displaying shorter chains. The main reaction products include the following species: ketones, acids, aldehydes and alcohols.<sup>22-25, 27, 31</sup>

The objective of this study is to deepen the knowledge of the thermo-oxidative mechanisms of liquid fuels. The complexity of the phenomena and their interactions require simplifying the approach and working on model molecules. The behavior of the constitutive molecules of Jet A-1 kerosene like linear alkane and monoaromatic will be evaluated. As Jet A-1 is a blend containing 40% of linear alkanes and 25% of 1, 2, 4-TriMethylBenzene (1,2,4-TMB), the behavior of pure *n*-dodecane and of 1,2,4-TMB subjected to autoxidative conditions will be first studied. In a second step, once the degradation mechanisms of these model molecules will be understood, it will be possible to blend them in proportions close to that of the Jet A-1 (80 % *n*-dodecane/20 % 1,2,4-TMB) to model a fuel surrogate.

## EXPERIMENTAL SECTION

### PetroOXY device

The PetroOXY device (Anton Paar) was used to carry out the oxidation stability studies (*Figure 2*). 5 mL of fuel are introduced into a glass crucible which is inserted into the hermetic chamber of the apparatus and subjected to a static pressure of pure oxygen of 700 kPa and heated up to 160 °C. The pressure and the temperature are measured continuously in the test cell. In this way, it is possible to follow the pressure decrease that reflects the oxygen consumption during the oxidation process, and thus the progress of the oxidation reaction. The ROOT method establishes the induction period (IP) defined as the time required to observe a pressure drop of 10 % compared to the maximum pressure observed, and therefore determine the overall kinetics of fuel oxidation. (*Figure 3*)

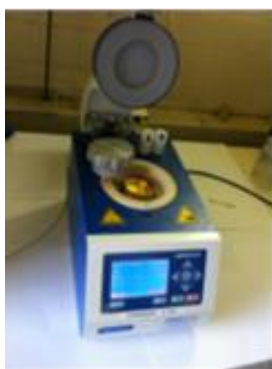


Figure 2- PetroOXY Device

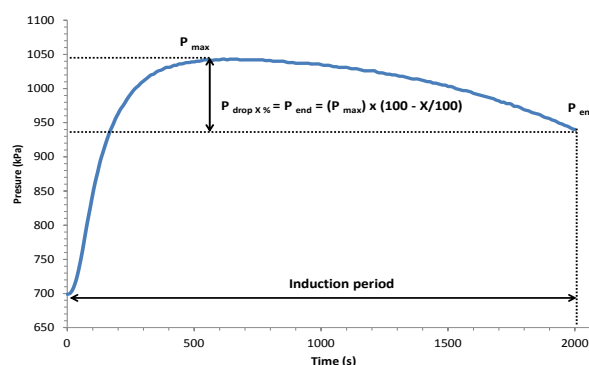


Figure 3 - Definition of the induction period

In order to emancipate from naturally dissolved oxygen molecules in the fuels and possible diffusion phenomena, the fuel is degassed in an ultrasonic bath for 2 minutes, in order to take into consideration only the pure oxygen introduced by the PetroOXY device.

In this study, the tests are performed for a fixed IP value for a pressure drop of 10 % in order to compare the stability to oxidation with a fixed initial pressure in pure oxygen of 700 kPa and at different temperatures: 140, 150 and 160 °C. All the oxidized samples were tested four times with this device to validate the repeatability of the tests.

At the end of a test and after cooling the device, the gaseous and liquid phases are recovered and analyzed.

### Characterization techniques

#### Analytical characterization

Gas phase analysis is performed using a Varian 4900 micro-GC. This equipment contains four analytical columns equipped with a Thermal Conductivity Detector (TCD). Each column is specific and permits to identify and quantify the gaseous products formed. It allows identifying gas products such as oxidized molecules (alcohols, aldehydes, ketones ...), shorts

alkanes (C<sub>2</sub> to C<sub>5</sub>), O<sub>2</sub>, H<sub>2</sub>, CO, CO<sub>2</sub> and CH<sub>4</sub> (carrier gas: He or Ar). Calibration is performed before each test. The dioxygen content is deduced from the volume of dioxygen initially introduced and the remaining content is detected in the gas phase.

Liquid phase oxidation products are analyzed by gas chromatography (GC) using a Varian 3900 chromatograph. This apparatus consists of an automatic sampler 8410, a fused silica capillary column (phase type: VF-5 ms), a FID detector, and the carrier gas is He. A temperature program has been optimized for the analysis of liquid products obtained for the model molecules. The consumption of hydrocarbon model molecules is followed by GC. Standard solutions are prepared by mixing different volumes of model fuel and a solvent to establish a calibration curve. Standard solutions and oxidized samples are injected at least three times and the chromatographic peak area differences must be less than 1% to validate the analysis. The identification of the species present in the liquid phase was carried out by analyses of gas chromatography coupled with mass spectroscopy (GC/MS) using a Varian 450 GC/320 MS chromatograph and with the same columns and temperature programs that were previously used on the Varian 3900. The MS fragmentation is performed by electronic impact of 70 eV.

At the end of a test, the liquid phase is collected and weighed. By this way, the quantification of the gas phase is carried out by determining the rates of gasification and dioxygen conversion.

The gasification rate of was calculated according to the formula:

$$\text{Gasification rate (\%)} = (m_i - m_f - m_s / m_i) \times 100$$

With:

m<sub>i</sub> : initial mass of model molecule introduced (g)

m<sub>f</sub> : final mass of the oxidized liquid phase recovered (g)

m<sub>s</sub> : mass of solid formed (g)

The dioxygen conversion rate was calculated using the following formula:

$$\text{Conversion rate of O}_2 \text{ (\%)} = (n_{i, \text{O}_2} - n_{f, \text{O}_2} / n_{i, \text{O}_2}) \times 100$$

With:

n<sub>i, O<sub>2</sub></sub>: initial quantity of dioxygen introduced into the PetroOXY chamber (mol)

n<sub>f, O<sub>2</sub></sub>: final quantity of dioxygen remaining in the gas phase (mol), which is found following the relation:

$$n_{f, \text{O}_2} \text{ (mol)} = n_{\text{Total gases}} - n_{\text{oxidized gases formed}}$$

The quantification of the liquid phase was carried out by determining the conversion rate of the pure molecules and calculated following the formula:

$$\text{Conversion rate of pure molecule (\%)} = (n_i - n_f / n_i) \times 100$$

## Chemical characterization

### Determination of the Peroxide Value (PV)

The quantification of the peroxide species formed in the liquid phase was carried out by the standardized method NF T 60-220<sup>32</sup> to obtain the peroxide value (PV). It is the number of milliequivalents of active oxygen present in peroxidic form, in a dm<sup>3</sup> of fuel. This method is based on titration by sodium thiosulphate solution of iodine molecules released by iodide oxidation by hydroperoxides samples.<sup>33</sup>

### Determination of Total Acid Number (TAN)

The total acid number (TAN) indicates the quantity of acid species present in sample<sup>2, 34</sup> and more exactly the mass of potassium hydroxide required to neutralize the free acid present in 1 g of fuel sample. The method used to determine the TAN is based on ASTM D3242.<sup>35</sup> The maximum allowable acidity for Jet A-1 kerosene is 0.10 mg KOH / g in ASTM D1655.<sup>36</sup>

### Measurement of water content

The water content was measured using a Karl-Fisher coulometer (Mettler Toledo C30). The principle of this device is based on coulometric titration. It allows the determination of small amounts of water in a sample by means of a current measurement during a quantitative reaction between water and iodine.

### Model molecules

*N*-Dodecane (> 99%) and 1, 2, 4-Trimethylbenzene (> 99%) were purchased from Alfa Aesar. The boiling point of these two molecules is 216.3 °C for *n*-dodecane and 169.0 °C for 1, 2, 4-TMB, which allows us to reach the high temperatures imposed by the PetroOXY device.

## RESULT AND DISCUSSION

### Evolution of the tests duration

The oxidation studies has been carried out using the PetroOXY device frequently used for oxidation stability studies of fuels and oils, in particular for small-scale rapid oxidation tests (ROOT) of fuels. This device has many advantages, such as working with a small sample volume while having good repeatability according to ASTM D7545<sup>37</sup> to study the oxidation stability of fuels.<sup>38-42</sup>

During a test, the evolution of the pressure over time is followed. It mainly corresponds to dioxygen consumption, related to the progress of the oxidation of the molecules but also to the formation of gaseous products. **Figure 4** presents the evolution curves of the pressure as a

function of time for the 2 model molecules and the blend. It shows that for a fixed temperature and initial pressure, the induction time is different and depending on the nature of the molecule.

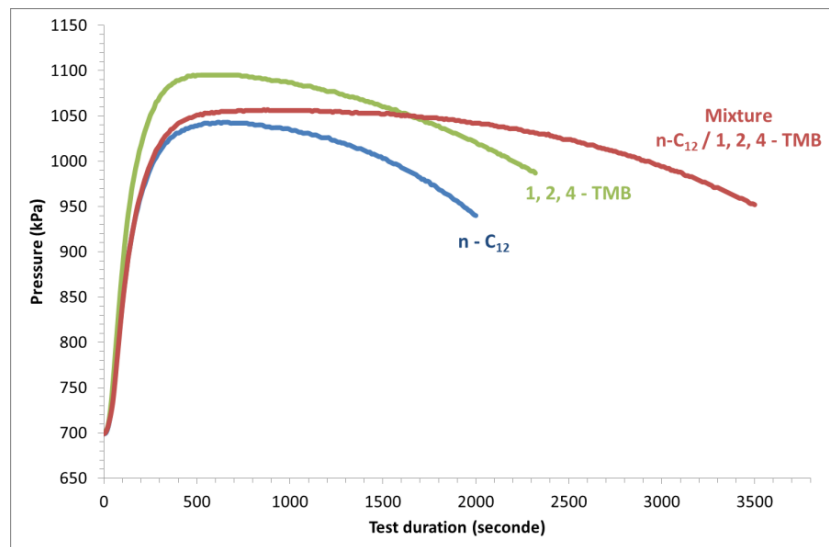


Figure 4 - Evolution of the dioxygen pressure as a function of time ( $T_i = 160\text{ }^\circ\text{C}$ ,  $P_{O_2} = 700\text{ kPa}$ )

The results summarizing the induction time are grouped together on **Table 1**. These results show that the induction time decreases with increasing temperature. This is consistent because temperature is a kinetic factor.

Table 1– Induction times for the two model molecules and the blend

	<b>n-C12</b>	<b>1, 2, 4 - TMB</b>	<b>Mixture n-C12 : 1, 2, 4- TMB</b>
Temperature ( $^\circ\text{C}$ )	Induction time (min)	Induction time (min)	Induction time (min)
140	159,88	147,88	281,90
150	67,63	71,38	114,75
160	32,72	36,08	54,44

In addition, in the *Figure 5*, the separately oxidized model molecules have relatively close induction times. However, when these two molecules are mixed, the induction time is longer. The fact that the behavior of the model molecules and that of the mixture is different highlights a possible interaction between the two model molecules.



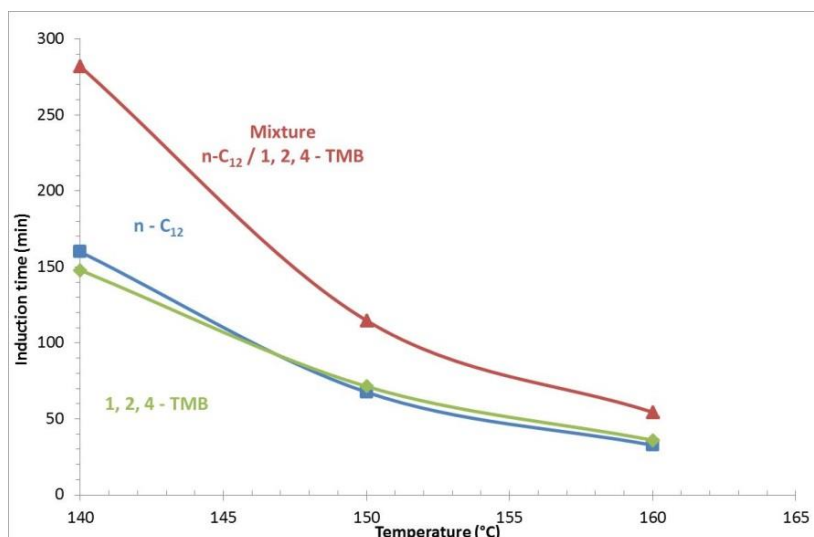


Figure 5 – Evolution of the induction times of the oxidation tests as a function of temperature

Based on the values presented on **Table 1** and the results presented in **Figure 5**, it appears that the induction time decrease the same way with the temperature for the two model molecules but faster for the blend.

### Gasification rate

Quantification of the gas phase formed is carried out by determining the rate of gasification. The results are grouped in **Table 2**. They show that the gasification rate seems to decrease with the temperature.

In addition, **Table 2** shows that oxidized *n*-dodecane has a 1% higher gasification rate than oxidized 1, 2, 4-TMB. This implies that a linear alkane molecule will produce more gaseous products than a monoaromatic molecule.

In the case of the mixture, it is interesting to note that the blend produces more gaseous products at low temperature than the two model molecules but less at high temperature.

Table 2- Gasification rate

	<b>n-C12</b>	<b>1, 2, 4 - TMB</b>	<b>Mixture n-C12 : 1, 2, 4-TMB</b>
Temperature (°C)	Gasification rate (%)	Gasification rate (%)	Gasification rate (%)
140	3,83	2,93	4,88
150	3,41	2,85	3,49
160	3,08	2,79	2,39

### Conversion rate of dioxygen

Quantification of the gas phase is completed by determining the conversion rate of dioxygen. The results are presented on **Figure 6** and show that the conversion rate increases with temperature.

In the case of model molecules, it has been observed that although the induction time is relatively close (**Table 1**), the conversion rates are different. This implies that for a given temperature, the conversion rate of the dioxygen depend on the nature of the molecule. Indeed, in the case of *n*-dodecane the conversion rate of dioxygen is 4 % higher than that of 1, 2, 4-TMB. This implies that the dioxygen consumption is higher for a linear alkane molecule than that for a monoaromatic molecule.

In the case of the mixture, an intermediate result is obtained, resulting from the proportion of the nature of the constituent molecules of the mixture.

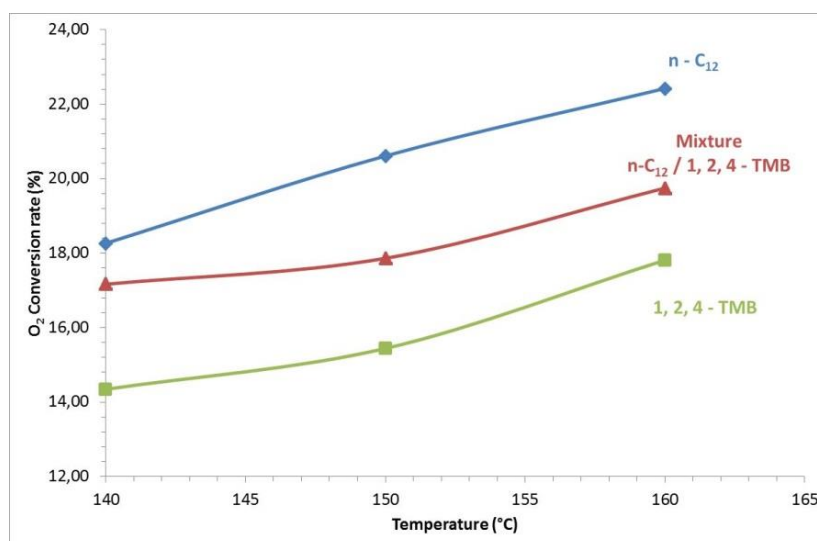


Figure 6 – Conversion rate of dioxygen

### Conversion rate of model molecules

The quantification of the liquid phase is carried out by evaluating the conversion rate of the model molecules. The results are presented in **Figure 7** which represents the conversion rate of model molecules according to the temperature.

In the case of the model molecules, it shows that their conversion rates increase with the temperature and that the conversion rate of 1, 2, 4-TMB is higher than that of the *n*-dodecane. According to the **Table 1**, the induction time of 1, 2, 4-TMB and *n*-dodecane are relatively close regardless of the temperature. This implies that for the same induction time, 1, 2, 4-TMB is more consumed than *n*-dodecane. Thus mono-aromatic molecules are more sensitive to oxidation than linear alkane molecules.

In the case of the blend, the inverse trend is observed. The conversion rate of the two reagents decreases, surprisingly with the temperature. The conversion rate of 1, 2, 4-TMB remains always higher than that of the *n*-dodecane.

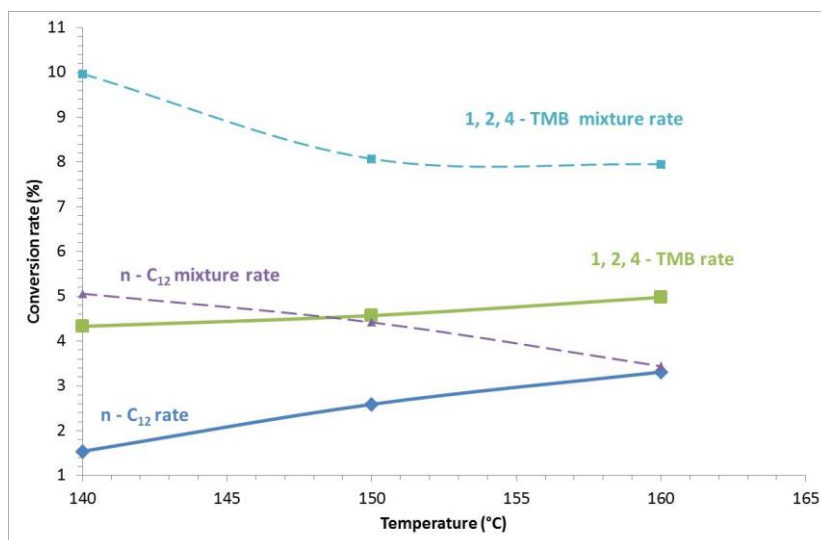


Figure 7- Conversion rate of model molecules (%)

The high consumption of dioxygen but the low conversion of pure *n*-dodecane would be explained by a highest reactivity of the secondary products than that the parent molecule. The dioxygen is more consumed during the formation of the secondary products as products carboxylic acids are formed. An opposite trend could be observed with the 1, 2, 4-TMB.

In the case of the blend, the conversion rate of the parent molecule seems to be exacerbated without important modification of the dioxygen consumption. Thus, the quantity of secondary products should be reduced and the induction time would increase as the first step of oxidation of the parent molecule is the slowest. With the increase of the temperature, the kinetics of the reactions are accelerated, the induction times are very close.

## Kinetics of dioxygen consumption and model molecules

### Kinetics of dioxygen consumption

Progress parameters studied previously made possible to highlight the kinetics of consumption of dioxygen, shown in *Figure 8*. This figure shows that the speed of consumption of dioxygen decreases with decreasing with temperature regardless of the model molecule studied.

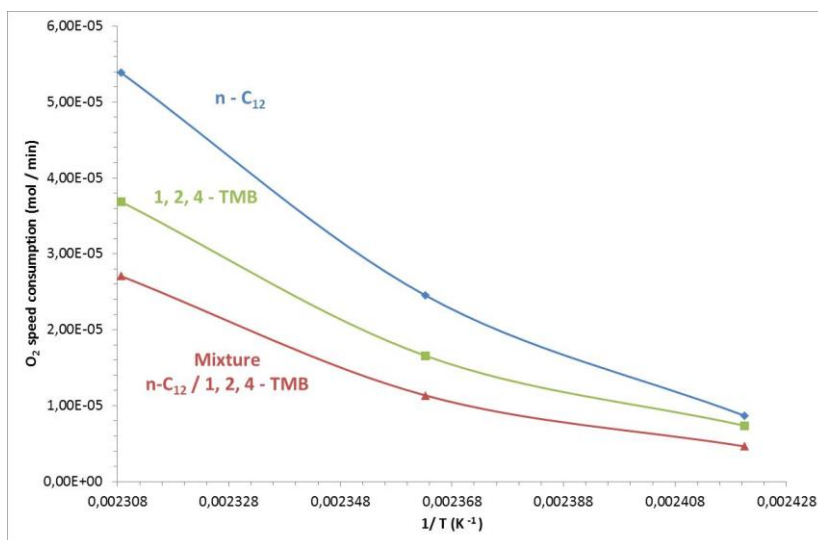


Figure 8 – Kinetic of dioxygen consumption

In the case of *n*-dodecane, the dioxygen is consumed more quickly than in the case of 1, 2, 4-TMB. This result is consistent with the result obtained on **Figure 6**. In addition, this figure highlights the fact that dioxygen is consumed less rapidly in the case of the mixture.

### Kinetics of consumption of model molecules

The kinetics of consumption of the model molecules has also been determined and is presented in **Figure 9**. The results show that the speed of consumption of the model molecules decreases with decreasing temperature. In addition, the kinetic consumption of the 1, 2, 4-TMB is higher than that of the *n*-dodecane. Thus the mono-aromatic are consumed much faster than the linear alkane. For the mixture the speed of consumption of the *n*-dodecane is equivalent to that of the 1, 2, 4-TMB. Moreover, being present in lower proportion initially (at 20% while *n*-dodecane is present at 80%), this may also explain the fact that it is consumed more slowly.

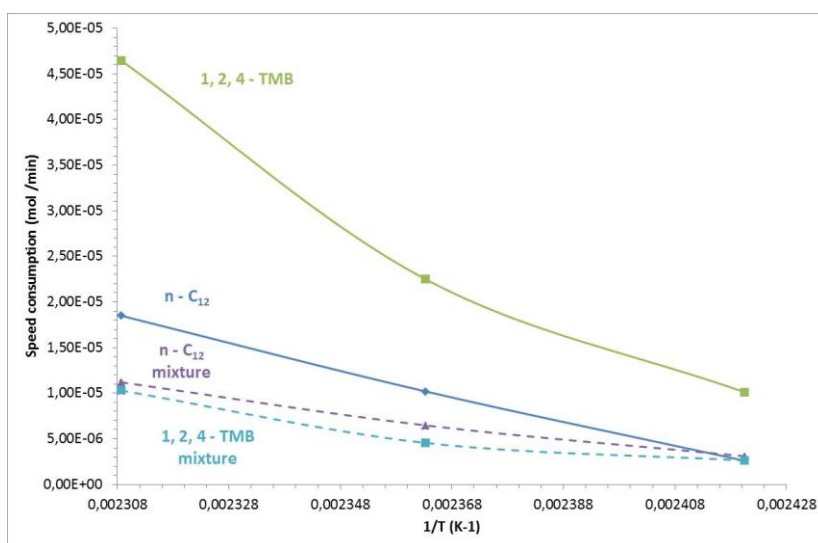


Figure 9 – Kinetics of consumption of oxidized model molecules

## Analysis of gas phase products

Gas phase analysis identified molecules such as H<sub>2</sub>, CO, CO<sub>2</sub>, short alkanes and alkenes from C<sub>2</sub> to C<sub>5</sub>, as shown in the chromatograms in **Figure 10**. The presence of CO<sub>2</sub> as well as short alkanes and alkenes induces the presence of a potential decarboxylation mechanism.

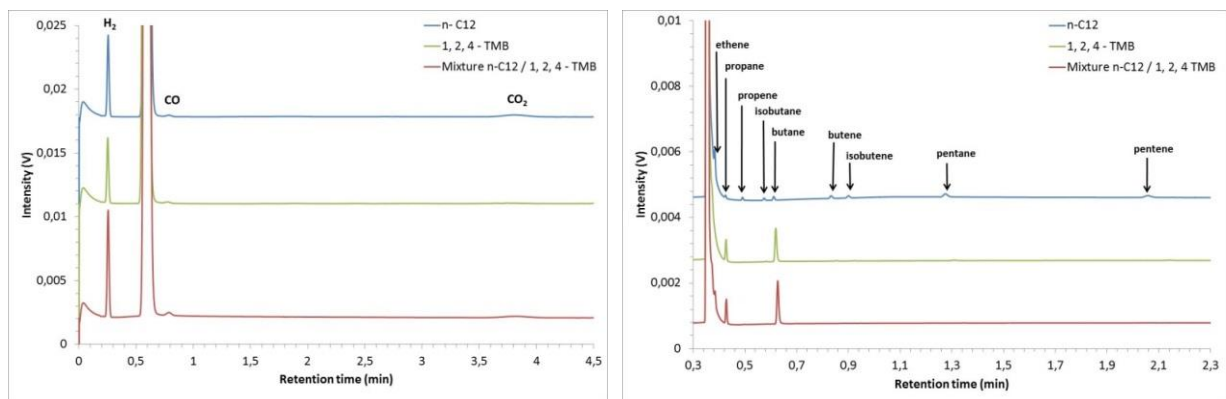


Figure 10 – Chromatograms of the gaseous phase ( $T_i = 160\text{ }^\circ\text{C}$ ,  $P_{O_2} = 700\text{ kPa}$ )

Quantification was carried out and is presented in **Figure 11**. This figure shows that the amount of gas decreases with increasing of the temperature. These results are in agreement with the gasification rates obtained and presented on **Table 2**.

It is noted that the amount of gas formed is greater in the case of 1, 2, 4-TMB.

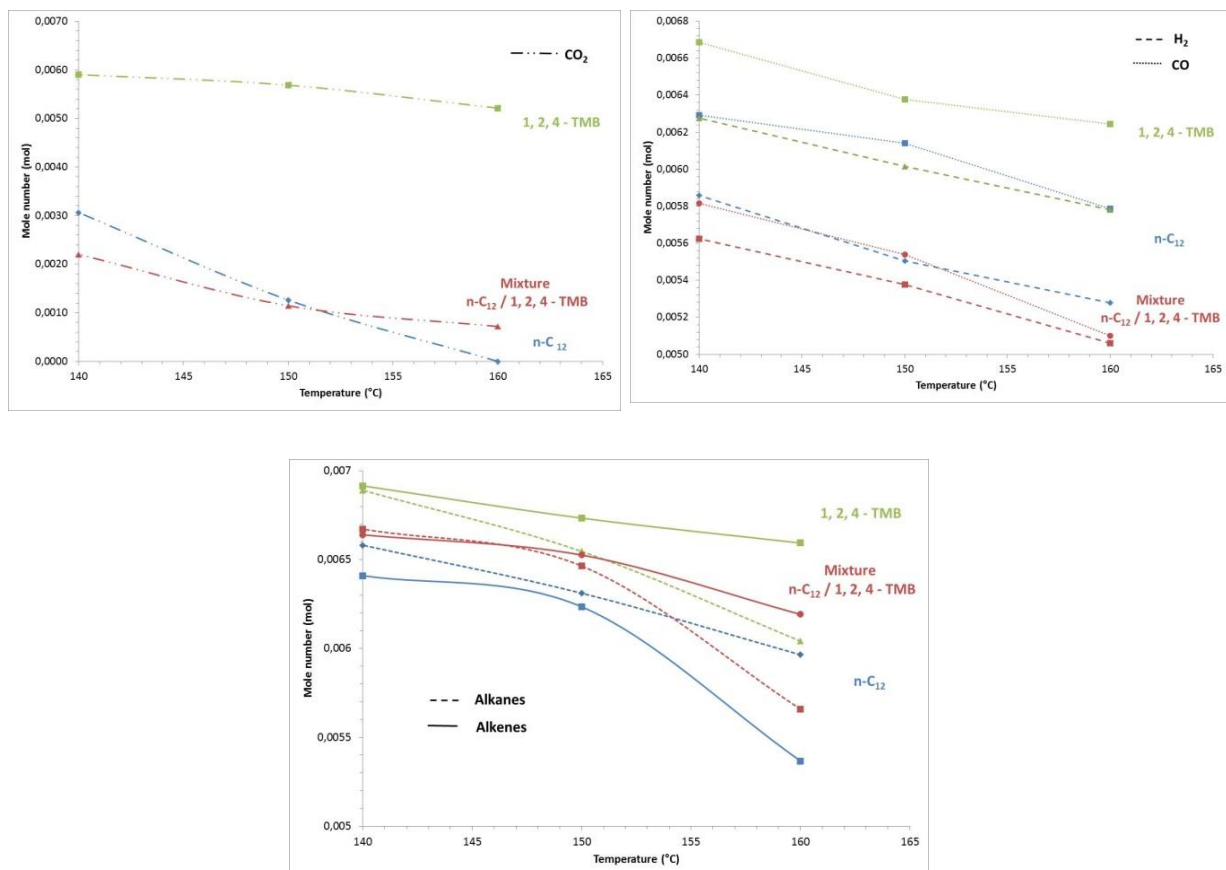


Figure 11 – Evolution of mole number of gaseous products as a function of temperature

## Analysis of liquid phase products

The GC analysis allowed to showing the pure reagent on the liquid phase before and after their oxidation. Before the oxidation, each molecule presents one characteristic peak. For the model molecules, the *n*-dodecane and the 1, 2, 4-TMB indicates one peak at 34 min and 27 min, respectively. For the blend, two peaks are presented characterizing the *n*-dodecane and the 1, 2, 4-TMB.

**Figure 12** shows the products formed after oxidation. In comparison with the pure reagents chromatogram result, some additional peaks are observed. These are oxidation products.

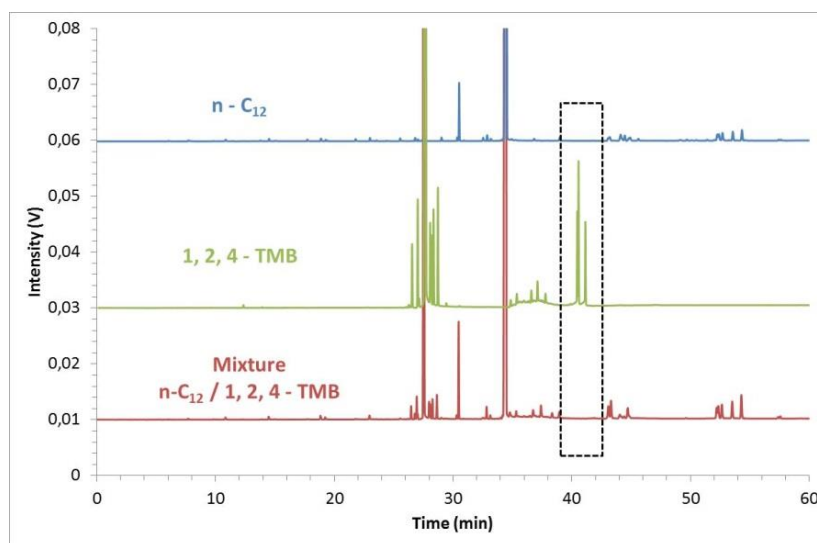


Figure 12 - GC chromatogram of the liquid phase products oxidized at 160 °C

For the blend, it is possible to note the presence of peaks, at the same retention times, as those present on the chromatogram of the model molecules. This indicates that the oxidation products formed in the case of the mixture are roughly the same as the molecules formed in the case of the oxidation of pure *n*-dodecane and 1,2,4-TMB.

The identification of these products has been done by GC/MS and shown that the products obtained in the liquid phase resulting from the oxidation of the two model molecules and of the mixture are: alcohols, carboxylic acids, ketones, aldehydes, benzenes alcohol, benzenes aldehyde, alkanes and aromatics hydrocarbon.

According to the literature, in the context of alkane autoxidation reactions, the ketone species are formed by a reaction of dismutation and hydrogen transfer reaction. In addition the  $\beta$ -scission reaction is dominant for alkoxy radicals. Therefore, the majority of alcoholic species are formed by dismutation reactions. It also helps to explain the low yield of alcohols compared to ketones and acids. Finally, the majority of organic acids are formed by the Baeyer-Villiger reaction pathways.<sup>25</sup>

However, some differences persist between the two model molecules concerning oxidized products formed. Indeed, on the chromatogram of 1, 2, 4-TMB, it is noted the presence of 3 peaks around 40 min. These peaks are absent in the mixture. GC/MS identification revealed that these were benzoic acid molecules as shown in **Figure 13**.

In addition, it is also interesting to note that the 1, 2, 4-TMB does not form ketones species, which induces that it promotes the oxidation of primary alcohols.

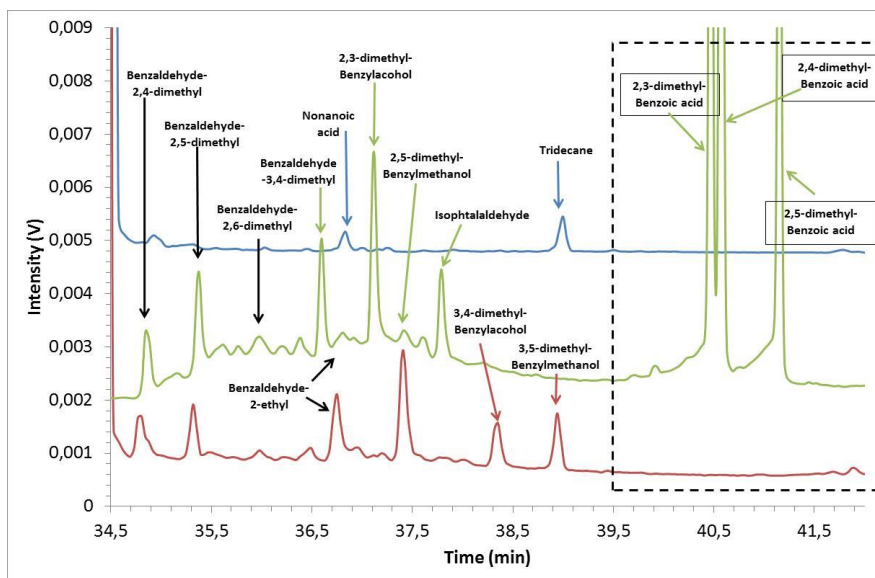
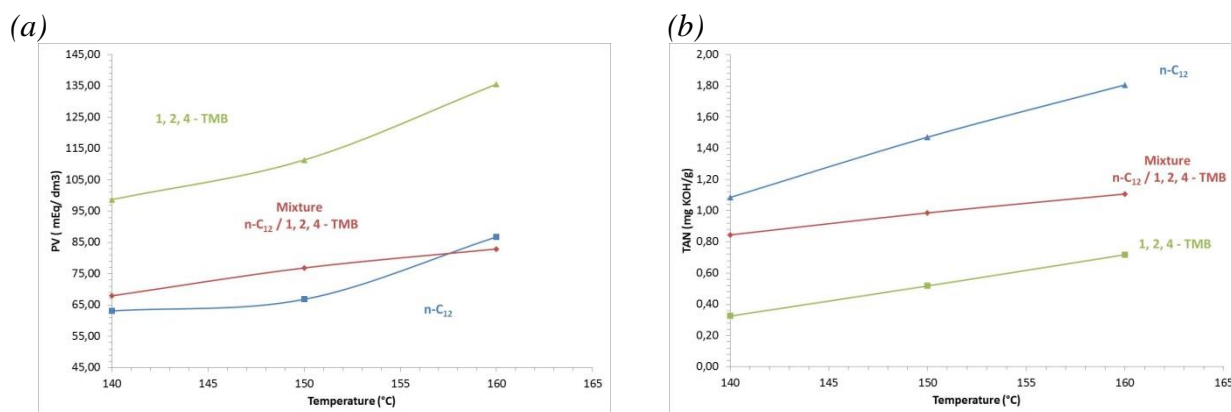
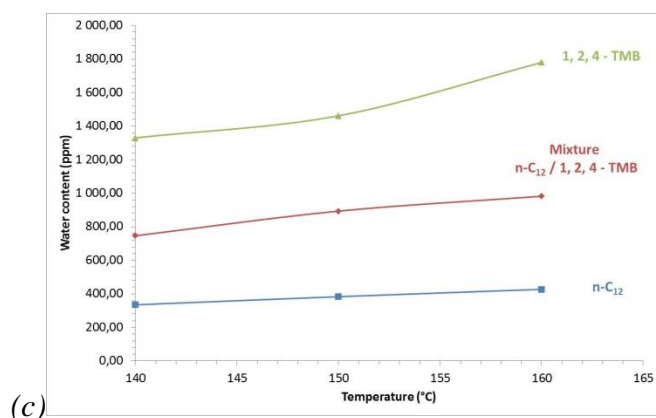


Figure 13 - Zoom of between 35 and 42 min of chromatogram of the oxidation of the liquid phase of the  $n\text{-C}_{12}$ , 1, 2, 4 - TMB and the mixture  $n\text{-C}_{12}/1,2, 4\text{-TMB}$  (80:20)

It is accepted that the peroxides species are the primary oxidation products. Thus they will be form and then will be decompose to interact and form the secondary oxidation products including the type species: ketones, acids and aldehydes. This is why it is interesting to also quantify the TAN number. The results are shown on the **Figure 14** - and it is another way to highlight the presence of liquid oxidized products characteristic of hydrocarbon oxidation. This shows the evolution of each of these parameters as a function of the temperature and that the amount of liquid oxidation products increases with temperature.





(c) *Figure 14 - Evolution of the parameters quantifying the formation of oxidation products as a function of temperature (a) the Peroxide Value, (b) the Total Acid Number and (c) the water content*

**Figure 14 (a)** shows the amount of PV formed during the oxidation reactions. It shows that the amount of PV formed by 1, 2, 4-TMB is higher than that of *n*-dodecane. **Figure 14 (b)** shows that TAN is higher in the case of *n*-dodecane oxidation than in the case of 1, 2, 4-TMB. This indicates that more acids species are produced during the oxidation of alkanes than in the case of monoaromatic molecules. This is confirmed by the GC/MS analysis, which further identifies a higher quantity of acid species during the oxidation of *n*-dodecane, especially the ketones species, which are absent during the oxidation of the 1, 2, 4-TMB. **Figure 14 (c)** shows that the water content is higher in the case of the 1, 2, 4-TMB than that of the *n*-dodecane. This can be explained by the fact that during the oxidation reaction of a primary alcohol, before forming a carboxylic acid, the latter oxidizes forming an aldehyde molecules and a water molecule <sup>43</sup>. According to **Figure 13**, the 1, 2, 4-TMB forms many benzene aldehyde species, and therefore, more generally, a higher amount of aldehyde, than the oxidized *n*-dodecane. This may explain the high water content observed in the case of 1, 2, 4-TMB oxidation.

### Analysis of the solid phase

At the end of a test, no solid phase was detected in the context of the oxidation of the model molecules.

However, in the case of the blend, the formation of a viscous and transparent gel was detected on the surface of the crucible in the form of a thin film. Unfortunately, this deposit could not be analyzed to the extent because it is formed in very small quantities.

## CONCLUSIONS

The aim of this study is the oxidation sensitivity of two model molecules: *n*-dodecane and 1, 2, 4-TMB, and their mixture (80:20 ratio respectively) using the PetroOXY device to compare their behavior under thermo-oxidative stress. The studies were carried out under dioxygen pressure of 700 kPa, with  $\Delta P$  of 10 % and at three different temperatures: 140, 150 and 160 °C. The results showed that the behavior of the molecules depends on the nature of the hydrocarbon families studied.



The first observation is that the alkanes and mono aromatics molecules have relatively similar induction times, whereas the blend of these two compounds induces an induction time twice as long. This result is interesting in that it reveals the presence of an interaction between the two molecules.

The second observation relates to the dioxygen conversion rates, which is higher in the case of *n*-dodecane. This is explained by the structure of the molecule. In fact, in the case of a linear alkane, the structure of the molecule has a long chain, so the dioxygen reacts more easily with the alkane, unlike the aromatic molecule where a steric gene is to be considered.

The last observation concerns the conversion rate of the model molecules. The results showed their conversion rates increase with the temperature and the conversion rate of 1, 2, 4-TMB was higher than that of *n*-dodecane. However, in the case of the blend, the conversion rate decreases with temperature.

The gas phase analyzes showed the formation of: H<sub>2</sub>, CO, short alkanes and alkenes from C<sub>2</sub> to C<sub>5</sub> and of CO<sub>2</sub>, showing the presence of a potential decarboxylation mechanism. The liquid analysis highlights the formation of different species depending to the nature of the model molecule. In the case of *n*-dodecane: alcohols, aldehydes, carboxylic acids, ketones, and alkanes are formed. In the case of the 1, 2, 4-TMB the analysis revealed the presence of aromatic hydrocarbon and oxidized benzene like benzene alcohol, benzene aldehyde and benzoic acid. In the case of the blend, all the molecules formed in the case of the model molecules are present with the exception of benzoic acid only present in the case of the oxidation of 1,2,4-TMB.

Finally, it has been observed the formation of a gel in the case of the mixture. This allows highlighting the interaction between linear alkanes and mono aromatic molecules. This phenomenon will be further characterized in future studies.

Other molecules will be studied alone or blended in order to identify their interactions between each other.

## REFERENCES

1. Grinstead B., Zabarnick, S., *Studies of Jet Fuel Thermal Stability, Oxidation, and Additives Using an Isothermal Oxidation Apparatus Equipped with an Oxygen Sensor*, Energy & Fuels 1999, 13, 756-760.
2. Pullen J., Saeed K., *An over view of biodiesel oxidation stability*, Renewable and Sustainable Energy Reviews, 2012, 16, 5924–5950.
3. Ervin J.S., Zabarnick S., *Computational Fluid Dynamics Simulations of Jet Fuel Oxidation Incorporating Pseudo-Detailed Chemical Kinetics*, Energy & Fuels 1998, 12, 344-352.
4. Jones E.G., Balster W.J., *Phenomenological Study of the Formation of Insolubles in a Jet-A Fuel*, Energy & Fuels 1993, 7, 968-977.
5. Jones E.G., Balster L.M., Balster W.J., *Autoxidation of Neat and Blended Aviation Fuels*, Energy & Fuels 1998, 12, 990-995.

6. Balster W.J., Jones E.G., *Effects of Temperature on Formation of Insolubles in Aviation Fuels*, Journal of Engineering for Gas Turbines and Power, 1998, 120, 289-293.
7. Ervin J.S., Williams T.F., *Dissolved Oxygen Concentration and Jet Fuel Deposition*, Ind. Eng. Chem. Res. 1996, 35, 899-904.
8. Jones E.G., *Autoxidation of Aviation Fuels in Heated Tubes: Surface Effects*, Energy & Fuels 1996, 10, 831-836.
9. Spadaccini L.J., Huang H., *On-Line Fuel Deoxygenation for Coke Suppression*, Journal of Engineering for Gas Turbines and Power, 2003, 125, 686-692.
10. Zabarnick S., *Chemical Kinetic Modeling of Jet Fuel Autoxidation and Antioxidant Chemistry*, Ind. Eng. Chem. Res. 1993, 32, 1012-1017.
11. Heneghan S.P., Zabarnick S., *Oxidation of jet fuels and the formation of Deposits*, Fuel, 1994, 73, p.1.
12. Kuprowicz N. J., Zabarnick S., West Z.J., Ervin J.S., *Use of Measured Species Class Concentrations with Chemical Kinetic Modeling for the Prediction of Autoxidation and Deposition of Jet Fuels*, Energy & Fuels 2007, 21, 530-544.
13. West, Dissertation: *Studies of jet fuel autoxidation chemistry: Catalytic hydroperoxides decomposition and high heat flux effects*, The School of Engineering of the University of Dayton, 2011 .
14. Mushrush G.W., Beal E.J., Slone E., Hardy D.R. *Reaction of organosulfur compounds with naturally occurring peroxides in jet fuel*, Energy & Fuels. 1996, 10, 504-508.
15. Wilson D.I., Watkinson A.P., *Chemical Reaction Fouling: A Review*, Experimental Thermal and Fluid Science, 1997, 14,361-374.
16. Warth V., Stef N., Glaude P.A., Battin-Leclerc F., Scacchi G., Côme G.M., *Computer-Aided Derivation of Gas-Phase Oxidation Mechanisms: Application to the Modeling of the Oxidation of n-Butane*, Combustion and Flame, 1998, 114, 81–102.
17. Waynick J.A., *Characterization of Biodiesel Oxidation and Oxidation products*, Fuels, Lubricants & Fluids Applications, 2005.
18. Ranzi E., Faravelli T., Gaffuri P., Garavaglia E., Goldaniga A., *Primary Pyrolysis and Oxidation Reactions of Linear and Branched Alkanes* Ind. Eng. Chem. Res. 1997, 36, 3336-3344.
19. Ranzi E., Cavallotti C., Cuoci A., Frassoldati A., Pelucchi M., Faravelli T., *New reaction classes in the kinetic modeling of low temperature oxidation of n-alkanes*, Combustion and Flame, 2015, 162 1679–1691.
20. Wang Z., Popolan-Vaida D. M., Chen B., Moshhammer K.G, Mohamed S. Y., Wang H., Sioud S., Raji M.A., Kohse-Höinghaus K., Hansen N., Dagaut P., Leone S. R., Sarathy S. M.,

*Unraveling the structure and chemical mechanisms of highly oxygenated intermediates in oxidation of organic compounds*, PNAS , 2017, 114, 50,13102–13107.

21. Jalan A., Alecu I.M., Meana-Pañeda R., Aguilera-Iparraguirre J., Yang K. R., Merchant S.S., Truhlar D. G., Green W. H., *New Pathways for Formation of Acids and Carbonyl Products in Low- Temperature Oxidation: The Korcek Decomposition of  $\gamma$ -Ketohydroperoxides*, J. Am. Chem. Soc. 2013, 135, 11100–11114.

22. Dounghthip, T., Ervin J., Zabarnick S., Williams T. *Simulation of the effect of metal-surface catalysis on the thermal oxidation of jet fuel*, Energy & Fuels, 2004, 18, 2, 425–437.

23. Garcia-Ochoa F., Romero A., Querol J., *Modeling of the Thermal n-Octane Oxidation in the Liquid Phase*, Ind. Eng. Chem. Res., 1989, 28, 43-48.

24. Câmara L.D.T., Monteiro R.S., Constantino A.M., Aranda D.A.G., Afonso J.C., *Oxidative Cracking of Linear Hydrocarbons at Low-*, Chemical Engineering Communications, 2010, 416-424.

25. Pfaendtner J., Broadbelt L. J., *Mechanistic Modeling of Lubricant Degradation. 2. The Autoxidation of Decane and Octane.*, Ind. Eng. Chem. Res., 2008, 47, 2897-2904.

26. Hazlett R. N., Hall J. M., Matson M., *Reactions of Aerated N-Dodecane Liquid Flowing over Heated Metal Tubes*, Ind. Eng. Chem., Prod. Res. Dev., 1977 16, 2, 171-177.

27. Boss B. D., Hazlett R. N., *Oxidation of hydrocarbons in the liquid phase: n-dodecane in a borosilicate glass chamber at 200°C*, Canadian Journal of Chemistry, 1969, 47, 4175-4182.

28. Boss B.D., Hazlett R.N., *n-Dodecane Oxidation-Elucidation by Internal Reference Techniques*, Ind. Eng. Chem., Prod. Res. Dev., 1975, 14, 2, 135-138.

29. Reddy K.T., Cernansky N. P., *Modified Reaction Mechanism of Aerated n –Dodecane Liquid Flowing over Heated Metal Tubes*, Energy & Fuels, 1988, 2, 205-213.

30. Blin-Simiand N., Jorand F., Sahetchian K., *Hydroperoxides With Zero, One, Two or More Carbonyl Groups Formed During the Oxidation of N-Dodecane*, Combustion and Flame, 2001, 126, 1524–1532.

31. Jensen R.K., Korcek S., Mahoney L. R., Zinbo M., *Elevated Temperatures. 1. The Stirred Flow Reactor Technique and Analysis of Primary Products from n-Hexadecane Autoxidation at 120-180 °C*, Journal of the American Chemical Society, 1979 ,101,25 ,7574-7584.

32. NF T 60-220 - *Corps gras d'origines animale et végétale. Détermination de l'indice de peroxyde*, 1995

33. NF EN ISO 660 - *Corps gras d'origine animale et végétale. Détermination de l'indice d'acide et d'acide*, 1999

34. Ashraful A.M., Masjuki H.H., Kalam M.A., Ashrafur Rahman S.M., Habibullah M., Syazwan M., *Study of the Effect of Storage Time on the Oxidation and Thermal Stability of Various Biodiesels and Their Blends*, Energy Fuels 2014, 28, 1081–1089.

35. ASTM D3242-08 - *Standard Test Method for Acidity in Aviation Turbine Fuel*.
36. ASTM D1655-18B - *Standard Specification for Aviation Turbine Fuels*.
37. ASTM D7545-09 *Standard Test Method for Oxidation Stability of Middle Distillate Fuels—Rapid Small Scale Oxidation Test (RSSOT)*.
38. Bacha K., Ben-Amara A., Vannier A., Alves-Fortunato M., Nardin M., *Oxidation Stability of Diesel/Biodiesel Fuels Measured by a PetroOxy Device and Characterization of Oxidation Products*, Energy Fuels, 2015, 29, 4345–4355.
39. Sicard, M.; Boulicault, J., Coulon, K., Thomasset, C., Ancelle, J., Raepsaet, B., and Ser, F. *Oxidation stability of jet fuel model molecules evaluated by rapid small scale oxidation tests. The 13th International Conference on Stability, Handling and Use of Liquid Fuels, IASH 2013*.
40. Araújo S.V., Rocha B.S., Luna F.M.T., Rola E. M. Azevedo D.C.S., Cavalcante C.L. *FTIR assessment of the oxidation process of castor oil FAME submitted to PetroOXY and Rancimat methods*, Fuel Processing Technology, 2011, 92, 1152–1155.
41. Chatelain K., Nicolle A., Ben Amara A., Catoire L., Starck L., *Wide Range Experimental and Kinetic Modeling Study of Chain Length Impact on n-Alkanes Autoxidation*, Energy Fuels, 2016, 30, 1294–1303.
42. Botella L., Bimbela F., Martín L., Arauzo J., Sánchez J.L., *Oxidation stability of biodiesel fuels and blends using the Rancimat and PetroOXY methods. Effect of 4-allyl-2,6-dimethoxyphenol and catechol as biodiesel additives on oxidation stability*, Frontiers in Chemistry, Chemical Engineering, 2014, 43, 2.
43. Marteau C., Ruyffelaere F., Aubry J. M., Penverne C., Favier D., Nardello-Rataj V., *Oxidative degradation of fragrant aldehydes, Autoxidation by molecular oxygen*, Tetrahedron, 2013, 69, 2268-2275.